C. elegans transgenerationally adapts to bacterial infection by increasing the expression of cysteine synthases in progeny

Nicholas O. Burton[1,*], Cristian Riccio[2,3], Alexandra Dallaire[2,4], Jon Price[2,4], Benjamin Jenkins[5], Albert Koulman[5], Eric A. Miska[2,3,4]

[1] Centre for Trophoblast Research, Department of Physiology, Development and Neuroscience, University of Cambridge, Cambridge, CB2 3EG, UK

[2]Gurdon Institute, University of Cambridge, Cambridge, CB2 1QN, UK

[3]Wellcome Sanger Institute, Wellcome Genome Campus, Cambridge CB10 1SA, UK

[4]Department of Genetics, University of Cambridge, Downing Street, Cambridge CB2 3EH, UK

[5] Metabolic Research Laboratories, University of Cambridge, Cambridge, CB2 0QQ, UK

[*]Correspondence: nob20@cam.ac.uk

Keywords
C. elegans, transgenerational inheritance, infection, pathogen, heritable, *rhy-1*, *cysl-1*, *cysl-2*, *wdr-23*

Abstract

Parental exposure to environmental stress can program adaptive changes in offspring development and physiology in diverse organisms (*1–4*). The mechanisms by which parental exposure to environmental stresses can program predictive adaptive responses in offspring remain almost completely unknown. Here we report that the soil bacteria *Pseudomonas vranovensis* is a natural pathogen of the nematode *Caenorhabditis elegans* and that parental exposure of *C. elegans* to *P. vranovensis* promotes offspring resistance to infection. This adaptation can be transmitted transgenerationally such that, under certain conditions, infection of adults can enhance the immunity of their descendants four generations later. We find that parental infection by *P. vranovensis* results in increased expression of the cysteine synthases CYSL-1 and CYSL-2 and the regulator of hypoxia inducible factor RHY-1 in progeny and show that the expression of these three genes in offspring is required for adaptation to *P. vranovensis.* Furthermore, we demonstrate that the expression of CYSL-1, CYSL-2, and RHY-1 is regulated by signalling via the WD40 repeat protein WDR-23. We speculate that analogous heritable regulation of gene expression controls other observations of parental environment programming changes in offspring physiology, including observations of parental exposure to pathogens priming offspring immunity (*4*).

Pathogens such as viruses, some bacteria and eukaryotes are among the most ubiquitous selection factors found in nature (*5*). To adapt to the constant threat of pathogens, diverse organisms have evolved mechanisms by which parental exposure to pathogens can prime offspring immunity (*4*, *6–11*). For example, in mammals, a mother can transfer specific antibodies to her offspring via milk to prime offspring immunity (*11*). Similar observations of parents priming offspring immunity in response to pathogens have been reported in both plants (*10*) and invertebrates (*6*), even though these organisms lack antibodies. These findings suggest that multiple independent mechanisms have evolved for parents to prime offspring immunity. The molecular mechanisms underlying antibody-independent heritable adaptations to pathogen infection remain unknown.

One of the major obstacles in determining the molecular mechanisms underlying heritable adaptations to pathogen infection is the lack of robust models that can be easily analyzed in the laboratory. To address this obstacle, we sought to develop a model of a heritable adaptation to bacterial infection in the nematode *C. elegans* by testing whether *C. elegans* could heritably adapt to potential bacterial pathogens from its natural environment. Previous sampling of bacterial species from the natural environments of *C. elegans* identified 49 as yet undescribed bacterial isolates that induce the expression of the immune response genes *irg-1* or *irg-5* (*12*). We tested whether parental exposure to these potentially pathogenic bacteria could enhance offspring survival in response to future exposure to the same bacteria. We found that parental exposure to two of the isolates, BIGb446 and BIGb468, significantly enhanced offspring survival in response to future exposure to the same bacteria (Fig. 1A). Specifically, approximately 95% of newly hatched larvae from parents fed a standard

laboratory diet of *E. coli* HB101 died within 24 hours of hatching on BIGb446 or BIGb468 (Fig. 1A). By contrast, 45% of embryos from adults briefly exposed to BIGb446 or BIGb468 were still alive at 24 hours (Fig. 1A) and a majority of these larvae survived through adulthood (Fig. 1, B and C). In addition, we found that adults were more resistant to BIGb446 than larval animals (Fig. S1A) and that UV-killed bacteria did not cause lethality (Fig. 1D). We conclude that parental exposure to bacterial isolates BIGb446 and BIGb468 enhances offspring survival in response to future exposure to these bacteria.

To determine the species identity of bacterial isolates BIGb446 and BIGb468 we performed long read whole genome sequencing and assembled the genomes of these bacteria. We found that the genomes of both BIGb446 and BIGb468 were approximately 5.9 Mb (Supplementary File 1 and 2) and were 99.38% identical across the entire genome (Table S1 and Fig. S2). We concluded that BIGb446 and BIGb468 are isolates of the same species. We compared the 16S rRNA sequence of BIGb446 to known bacterial genomes using BLAST. We found that the 16s rRNA sequence from BIGb446 is 99.93% identical to *Pseudomonas vranovensis* strain 15D11. Previous studies of *Pseudomonas* phylogeny have used the DNA sequences of *gyrB*, *rpoB*, and *recA* to differentiate species of *Pseudomonas,* with similarity above 97% set as the accepted species threshold (*13*, *14*). We found that the sequence of *gyrB* was 98.05% identical, the sequence of *rpoB* was 99.44% identical, and the sequence of *recA* was 98.66% identical to the sequences of homologous genes in *P. vranovensis* strain 15D11. No other species of *Pseudomonas* was greater than 97% identical to *Pseudomonas sp.* BIGb446 at any of these three genes. Furthermore, we compared the average nucleotide identity (ANI) of our assembly of *Pseudomonas sp.* BIGb446 with the genome of *P. vranovensis* strain 15D11 using OrthoANIu (*15*). We found these two genomes had an average nucleotide identity of

97.33%. We conclude that *Pseudomonas sp.* BIGb446 and *Pseudomonas sp.* BIGb468 are isolates of *Pseudomonas vranovensis*, a Gram-negative soil bacterium (*16*).

In some cases, the effects of parental stress on offspring have been reported to be intergenerational and only last a single generation (*1*). In other cases, the effects of parental stress on offspring have been reported to persist transgenerationally and thus affect descendants several generations later (*17–19*). To test whether exposure to BIGb446 had any transgenerational effects on immunity we fed adult animals BIGb446 for 24 hours and assayed the response of progeny two generations later. We found that a single exposure of adult animals to BIGb446 enhanced their offspring's survival (one generation later) but did not enhance the survival of their descendants two generations later (Fig. 1E), indicating that the effects of parental exposure to BIGb446 only last a single generation under these conditions. Some studies of the effects of parental environment on offspring have found that consecutive exposure of multiple generations of animals to the same stress can enhance adaptation to stress in descendants (*18*). We therefore tested whether the exposure of five consecutive generations (P0, F1, F2, F3, and F4) of animals to BIGb446 could enhance progeny (F5) survival in response to BIGb446 but found that this was not the case (Fig. 1E). Finally, we tested whether the exposure of four consecutive generations of animals to BIGb446 could enhance survival in progeny for more than a single generation. Unlike a single generation of exposure to BIGb446, we found that the enhanced survival of descendants of animals exposed to BIGb446 for four consecutive generations persisted for two generations (Fig. 1E). Furthermore, we found that three consecutive generations of exposure to BIGb446 was required for resistance to BIGb446 to persist transgenerationally (Fig. 1F). We conclude that under conditions of multiple consecutive generations of animals

being exposed to BIGb446 the effects of exposure to BIGb446 can be transmitted transgenerationally.

Multiple signaling pathways and epigenetic modifiers have been proposed to mediate heritable and transgenerational responses to environmental stress. We tested whether mutations in any factors previously reported to be involved heritable or transgenerational responses to stress were required for *C. elegans* heritable adaptation to BIGb446 including small RNA mediated pathways (*hrde-1* (*20*), *prg-1* (*19*)), H3K9 methylation (*set-32* (*21*) and *met-2* (*22*)), H3K4 methylations (*set-2, wdr-5.1, spr-5*) (*17, 18*), DNA adenosine methylation (*damt-1*) (*18*), and the RAS/ERK signaling pathway (*lin-45*) (*1*). We found that none of these factors were required for *C. elegans* adaptation to BIGb446 (Fig. S1B) These data suggest that adaptation to *P. vranovensis* involves an as yet unknown mechanism of inheritance.

Bacterial isolates BIGb446 and BIGb468 were originally reported to promote the expression of immune response gene *irg-5* (*12*). The expression of *irg-5* in response to pathogen infection is controlled by the p38-like MAP kinase PMK-1 (*23*). We tested whether PMK-1 is required for resistance to BIGb446 by placing wild-type and *pmk-1* mutant adults on plates seeded with BIGb446. We found that 100% of *pmk-1* mutants were dead after 48 hours while more than 40% of wild-type animals remained alive (Fig. S1A). These results indicate that PMK-1 promotes resistance to BIGb446. We tested whether PMK-1 was required for heritable adaptation to BIGb446 by exposing wild-type and *pmk-1* mutants to BIGb446 for 24 hours and assaying the survival of their offspring in response to repeated exposure to BIGb446. We found that PMK-1 is not required for the heritable adaptation to BIGb446 (Fig. S1C).

C. elegans' heritable adaptation to *P. vranovensis* might be a general response to pathogen infection or specific to *P. vranovensis.* To test whether parental infection by different bacterial pathogens could protect offspring from BIGb446 we exposed adult animals to two additional bacterial pathogens of *C. elegans*, *Pseudomonas aeruginosa* PA14 (*24*) and *Photorhabdus luminescens* Hb (*25*), and assayed the response of their offspring to BIGb446. We found that parental infection by these two pathogens did not enhance offspring survival in response to BIGb446 (Fig. 1G). These results indicate that adaptation to *P. vranovensis* is not a generic response to pathogenic bacteria.

Previous studies found that *C. elegans* can heritably adapt to osmotic stress and starvation by regulating gene expression and metabolism in offspring (*1*, *26*). To identify how parental infection by BIGb446 affects gene expression and metabolism in offspring we profiled gene expression by RNA-seq and metabolite levels by LC/MS. Using RNA-seq we identified 1,153 genes that exhibit increased expression greater than 2-fold and 491 genes that decreased expression greater than 2-fold in embryos from parents fed BIGb446 when compared to embryos from parents fed HB101 (Fig. 2A and Table S2). We also quantified gene expression in young adults exposed to BIGb446. We found that 1,275 genes exhibited a greater than 2-fold change in expression when compared to young adults fed HB101 (Table S2). Of these 1,275 genes, 398 were also observed to change in embryos (Fig. 2B). We conclude that infection by *P. vranovensis* BIGb446 results in similar, but distinct, effects on adult and embryonic gene expression. Using LC/MS we profiled 92 lipid metabolites, including those previously observed to heritably change in abundance in response to osmotic stress (*27*), and found that 6 metabolites exhibit modest changes in abundance in embryos from parents fed BIGb446 when compared to embryos from parents fed HB101 (Fig. 2C and

Table S3). We conclude that parental exposure to the pathogenic diet of *P. vranovensis* BIGb446 alters gene expression and metabolite abundance in embryos.

We previously found that parental infection by *P. aeruginosa* PA14 and *P. luminescens* Hb did not protect offspring from BIGb446 (Fig. 1G). We hypothesized that different parental infections might result in different gene expression and metabolite changes in embryos and that the specific changes caused by parental infection by BIGb446 are required for offspring adaptation to BIGb446. To compare how parental infection by different bacterial pathogens affects offspring gene expression and metabolism we exposed young adults to *P. aeruginosa* PA14 or *P. luminescens* Hb for 24 hours and collected embryos from these animals to profile gene expression by RNA-seq and metabolites by LC/MS. We found that only 41 genes exhibited a greater than 2-fold change in expression in embryos from parents exposed to PA14 when compared to embryos from parents exposed to HB101 and of these genes 29 also exhibited altered gene expression in embryos from parents exposed to BIGb446 (Fig. 2, D and E, Table S4). Separately, we found that only 26 genes exhibited a greater than 2-fold change in expression in embryos from parents exposed to *P. luminescens Hb* when compared to parents fed HB101 (Fig. 2, D and E, Table S4). Of these genes, only 5 also exhibited altered expression in embryos from parents exposed to BIGb446 (Fig. 2D). Collectively, these results indicate that parental infection by *P. aeruginosa* and *P. luminescens* had only a limited effect on offspring gene expression when compared to parental infection by *P. vranovensis*. Only a single lipid metabolite measured exhibited a statistically significant change in abundance in embryos from parents fed *P. aeruginosa* and *P. luminescens* (Table S3). We conclude that parental exposure to different pathogenic diets has distinct effects on offspring gene expression.

We hypothesized that the specific changes in gene expression in embryos from parents exposed to *P. vranovensis* BIGb446 mediate the observed adaptation to this pathogen. Among the genes that we found to specifically increase in expression in response to BIGb446 was the glutathione-s-transferase *gst-31* (among the top 10 most upregulated genes (Table S2)) and we confirmed that *C. elegans'* exposure to BIGb446 resulted in increased expression of *gst-31* in both adults and embryos using a GFP reporter (Fig. 3, A and B). To identify factors that regulate animals' gene expression in response to BIGb446 we performed a chemical mutagenesis screen for mutants that exhibit increased expression of *gst-31* even when fed a normal laboratory diet of *E. coli* HB101. We identified four mutants from this screen and all four contain mutations in the conserved WD40 repeat protein *wdr-23* (Fig. 3C). Consistent with our findings, multiple previous studies have identified that *wdr-23* mutants exhibit increased expression of glutathione-s-transferases, including *gst-31* (*28–30*). We conclude that WDR-23 negatively regulates the expression of *gst-31*.

We tested whether the loss of WDR-23 affected *C. elegans* adaptation to *P. vranovensis* and found that multiple independent *wdr-23* mutants were unable to heritably adapt to BIGb446 (Fig. 3D). These results indicate that loss of WDR-23 prevents animals from being able to adapt to BIGb446. WDR-23 is a negative regulator of the Nrf2-like transcription factor SKN-1 and the loss of WDR-23 results in SKN-1 activation (*31*). Activation of SKN-1 in turn promotes the expression of oxidative stress response genes (*30*) and mutations in *skn-1* suppress many of the defects observed in *wdr-23* mutants (*31*). We exposed wild-type, *skn-1* partial loss-of-function, and *wdr-23;skn-1* double mutant adults to BIGb446 and assayed the response of their offspring to BIGb446. We found that partial loss-of-function mutations in *skn-1* (null mutants are embryonic lethal) also reduced animals' ability to adapt to BIGb446 and that this mutation in *skn-1* did not suppress the adaptation defect of *wdr-23* mutants (Fig.

3D). Collectively, these results indicate that mutations that both increase and decrease the activity of SKN-1 disrupt animals' ability to adapt to *P. vranovensis.* We propose that proper signaling via WDR-23 and SKN-1 is critical for *C. elegans* to adapt to *P. vranovensis.*

We previously observed that parental exposure to BIGb446 modifies gene expression in offspring. We hypothesized that parental infection by BIGb446 might regulate the expression of pathogen or stress response genes in offspring via WDR-23 and SKN-1. To test this hypothesis, we first performed RNA-seq of wild-type and *wdr-23* mutant embryos. We identified that 1,634 genes exhibited a greater than 2-fold change in expression in *wdr-23* mutants (Fig. 3E and Table S5). Of these genes, we found that 634 also exhibit a greater than 2-fold change in expression in embryos from parents exposed to BIGb446 (Fig. 3E and Table S5). Despite regulating an overlapping set of genes, we found that parental exposure to BIGb446 and the loss of WDR-23 resulted in distinct gene expression patterns (Fig. 3F). These data indicate that exposure to *P. vranovensis* and signaling via WDR-23 regulate the expression of a significantly overlapping set of target genes and are consistent with our hypothesis that parental exposure to BIGb446 modifies gene expression in offspring in part via WDR-23.

A large majority of genes that exhibit a greater than 2-fold change in expression in response to *P. vranovensis* or loss of WDR-23 exhibit an increase in mRNA expression (Table S5). We compared lists of genes exhibiting a greater than 5-fold increase in expression in both *wdr-23* mutant embryos and wild-type embryos from parents exposed to BIGb446. Of the 43 genes that exhibit a greater than 5-fold increase in expression in both conditions, two genes, *rhy-1* and *cysl-2*, were previously found to function in the same signaling pathway that regulates animals' response to resistance to hypoxic stress (Fig. 4, A and B), and we

confirmed that exposure of parents to BIGb446 increases CYSL-2 expression in embryos using a GFP reporter (Fig. 4C) (*32*). We hypothesized that increased expression of *rhy-1* and *cysl-2* in offspring promotes adaptation to *P. vranovensis*. We assayed three independent mutants lacking *rhy-1* and two independent mutants lacking *cysl-2* and found that these mutants were unable to adapt to BIGb446 (Fig. 4, D and E and Fig. S3). In addition, we found that these defects could be rescued by expressing wild-type copies of *rhy-1* and *cysl-2*, respectively (Fig. 4, D and E). We conclude that RHY-1 and CYSL-2 are required for adaptation to BIGb446.

RHY-1 and CYSL-2 were previously found to function in a signaling pathway with the CYSL-2 paralog, CYSL-1, the EGLN1 homolog EGL-9, and the hypoxia inducible factor HIF-1 to regulate animals' response to hypoxia (*32*). We tested whether mutants lacking CYSL-1, EGL-9, and HIF-1 also exhibited altered adaptation to BIGb446. We found that seven independent mutations in *cysl-1* resulted in animals that did not adapt to BIGb446 (Fig. 4F and Fig. S3), similar to *rhy-1* and *cysl-2* mutants. By contrast, we found that the loss of *hif-1* and *egl-9* did not affect adaptation to BIGb446 (Fig. 4G). These results indicate that RHY-1, CYSL-1, and CYSL-2 function separately from EGL-9 and HIF-1 to promote animals' adaptation to *P. vranovensis.*

Collectively, our results demonstrate that *P. vranovensis* is a pathogen of *C. elegans* and that parental exposure of *C. elegans* to *P. vranovensis* can protect offspring from future infection by increasing the expression of the cysteine synthases *cysl-1* and *cysl-2* and the regulator of hypoxia inducible factor *rhy-1* in progeny. The expression of *cysl-1*, *cysl-2* and *rhy-1* is regulated by signaling via WDR-23, however, we found that mutations that both increase and decrease SKN-1 activity disrupt adaptation to *P. vranovensis.* We propose that specific

signaling via WDR-23 and SKN-1, likely in combination with signaling via other pathogen response pathways, is required to elicit a distinct response to *P. vranovensis* and that completely abolishing signalling via this pathway using genetic mutants results in an inappropriate response to *P. vranovensis* and animals that are unable to adapt. Such a model is similar to other core signaling pathways that regulate animals' response to multiple different stresses, such as the insulin-like signaling pathway in *C. elegans* that functions in combination with signaling via SSU-1 and NHR-1 to specify *C. elegans* distinct responses to both starvation and osmotic stress (*27*).

The ability of *P. vranovensis* to kill *C. elegans* larvae within 24 hours and the observation that *C. elegans* activates genes associated with oxidative stress in response to *P. vranovensis* suggests that *P. vranovensis* produces a toxic molecule(s) that is lethal to *C. elegans*. The cysteine synthases CYSL-1 and CYSL-2 have been reported to break down toxic molecules such as hydrogen cyanide and hydrogen sulfide (*33*). We propose that *C. elegans* can transgenerationally adapt to infection *by P. vranovensis* by increasing the expression of CYSL-1 and CYSL-2 in offspring which protects animals by breaking down bacterial toxins. Thus, we demonstrate a new transgenerationally adaptive mechanism for *C. elegans* to fight a natural pathogen.

References and Notes:

1. N. O. Burton *et al.*, Insulin-like signalling to the maternal germline controls progeny response to osmotic stress. *Nat. Cell Biol.* **19**, 252–257 (2017).

2. B. Dantzer *et al.*, Density triggers maternal hormones that increase adaptive offspring growth in a wild mammal. *Science*. **340**, 1215–1217 (2013).

3. N. N. Vellichirammal, P. Gupta, T. A. Hall, J. A. Brisson, Ecdysone signaling underlies the pea aphid transgenerational wing polyphenism. *Proc. Natl. Acad. Sci. U. S. A.* **114**, 1419–1423 (2017).

4. O. Roth *et al.*, Paternally derived immune priming for offspring in the red flour beetle, *Tribolium castaneum*. *J. Anim. Ecol.* **79**, 403–413 (2010).

5. W. D. Hamilton, R. Axelrod, R. Tanese, Sexual reproduction as an adaptation to resist parasites (a review). *Proc. Natl. Acad. Sci. U. S. A.* **87**, 3566–3573 (1990).

6. T. J. Little, A. R. Kraaijeveld, Ecological and evolutionary implications of immunological priming in invertebrates. *Trends Ecol. Evol.* **19**, 58–60 (2004).

7. J. Dhinaut, M. Chogne, Y. Moret, Immune priming specificity within and across generations reveals the range of pathogens affecting evolution of immunity in an insect. *J. Anim. Ecol.* **87**, 448–463 (2018).

8. F. Yue *et al.*, Maternal transfer of immunity in scallop *Chlamys farreri* and its trans-generational immune protection to offspring against bacterial challenge. *Dev. Comp. Immunol.* **41**, 569–577 (2013).

9. C. C. Huang, Y. L. Song, Maternal transmission of immunity to white spot syndrome associated virus (WSSV) in shrimp (*Penaeus monodon*). *Dev. Comp. Immunol.* **23**, 545–552 (1999).

10. E. Luna, T. J. A. Bruce, M. R. Roberts, V. Flors, J. Ton, Next-generation systemic acquired resistance. *Plant Physiol.* **158**, 844–853 (2012).

11. L. A. Hanson *et al.*, The transfer of immunity from mother to child. *Ann. N. Y. Acad. Sci.* **987**, 199–206 (2003).

12. B. S. Samuel, H. Rowedder, C. Braendle, M.-A. Felix, G. Ruvkun, *Caenorhabditis elegans* responses to bacteria from its natural habitats. *Proc. Natl. Acad. Sci. U. S. A.* **113**, E3941-3949 (2016).

13. M. Gomila, A. Pena, M. Mulet, J. Lalucat, E. Garcia-Valdes, Phylogenomics and systematics in *Pseudomonas*. *Front. Microbiol.* **6**, 214 (2015).

14. P. N. Tran, M. A. Savka, H. M. Gan, In-silico taxonomic classification of 373 genomes reveals species misidentification and new genospecies within the genus *Pseudomonas*. *Front. Microbiol.* **8**, 1296 (2017).

15. S.-H. Yoon, S.-M. Ha, J. Lim, S. Kwon, J. Chun, A large-scale evaluation of algorithms to calculate average nucleotide identity. *Antonie Van Leeuwenhoek*. **110**, 1281–1286 (2017).

16. L. Tvrzova *et al.*, *Pseudomonas moraviensis sp. nov.* and *Pseudomonas vranovensis sp. nov.*, soil bacteria isolated on nitroaromatic compounds, and emended description of *Pseudomonas asplenii. Int. J. Syst. Evol. Microbiol.* **56**, 2657–2663 (2006).

17. E. L. Greer *et al.*, Transgenerational epigenetic inheritance of longevity in *Caenorhabditis elegans. Nature*. **479**, 365–371 (2011).

18. C. Ma *et al.*, N6-methyldeoxyadenine is a transgenerational epigenetic signal for mitochondrial stress adaptation. *Nat. Cell Biol.* **21**, 319–327 (2019).

19. R. S. Moore, R. Kaletsky, C. T. Murphy, Piwi/PRG-1 Argonaute and TGF-β Mediate Transgenerational Learned Pathogenic Avoidance. *Cell* (2019), doi:10.1016/j.cell.2019.05.024.

20. B. A. Buckley *et al.*, A nuclear Argonaute promotes multigenerational epigenetic inheritance and germline immortality. *Nature*. **489**, 447–451 (2012).

21. A. Ashe *et al.*, piRNAs can trigger a multigenerational epigenetic memory in the germline of *C. elegans*. *Cell*. **150**, 88–99 (2012).

22. I. Lev *et al.*, MET-2-Dependent H3K9 methylation suppresses transgenerational small RNA inheritance. *Curr. Biol. CB*. **27**, 1138–1147 (2017).

23. D. D. Bolz, J. L. Tenor, A. Aballay, A conserved PMK-1/p38 MAPK is required in *Caenorhabditis elegans* tissue-specific immune response to *Yersinia pestis* infection. *J. Biol. Chem.* **285**, 10832–10840 (2010).

24. D. H. Kim *et al.*, A conserved p38 MAP kinase pathway in *Caenorhabditis elegans* innate immunity. *Science*. **297**, 623–626 (2002).

25. I. Engelmann *et al.*, A comprehensive analysis of gene expression changes provoked by bacterial and fungal infection in *C. elegans. PloS One*. **6**, e19055 (2011).

26. M. A. Jobson *et al.*, Transgenerational Effects of Early Life Starvation on Growth, Reproduction, and Stress Resistance in *Caenorhabditis elegans. Genetics*. **201**, 201–212 (2015).

27. N. O. Burton *et al.*, Neurohormonal signaling via a sulfotransferase antagonizes insulin-like signaling to regulate a *Caenorhabditis elegans* stress response. *Nat. Commun.* **9**, 5152 (2018)

28. L. Tang, W. Dodd, K. Choe, Isolation of a hypomorphic *skn-1* allele that does not require a balancer for maintenance. *G3 Bethesda Md*. **6**, 551–558 (2015).

29. T. A. Staab *et al.*, The conserved SKN-1/Nrf2 stress response pathway regulates synaptic function in *Caenorhabditis elegans. PLoS Genet.* **9**, e1003354 (2013).

30. Z. Xu *et al.*, WDR-23 and SKN-1/Nrf2 Coordinate with the BLI-3 Dual Oxidase in Response to Iodide-Triggered Oxidative Stress. *G3 Bethesda Md*. **8**, 3515–3527 (2018).

31. K. P. Choe, A. J. Przybysz, K. Strange, The WD40 repeat protein WDR-23 functions with the CUL4/DDB1 ubiquitin ligase to regulate nuclear abundance and activity of SKN-1 in *Caenorhabditis elegans. Mol. Cell. Biol.* **29**, 2704–2715 (2009).

32. D. K. Ma, R. Vozdek, N. Bhatla, H. R. Horvitz, CYSL-1 interacts with the O2-sensing hydroxylase EGL-9 to promote H2S-modulated hypoxia-induced behavioral plasticity in *C. elegans. Neuron*. **73**, 925–940 (2012).

33. M. W. Budde, M. B. Roth, The response of *Caenorhabditis elegans* to hydrogen sulfide and hydrogen cyanide. *Genetics*. **189**, 521–532 (2011).

34. S. Brenner, The genetics of *Caenorhabditis elegans. Genetics*. **77**, 71–94 (1974).

35. S. Kurtz *et al.*, Versatile and open software for comparing large genomes. *Genome Biol.* **5**, R12 (2004).

36. J. Folch, M. Lees, G. H. Sloane Stanley, A simple method for the isolation and purification of total lipides from animal tissues. *J. Biol. Chem.* **226**, 497–509 (1957).

37. S. Virtue *et al.*, Peroxisome Proliferator-Activated Receptor gamma2 Controls the Rate of Adipose Tissue Lipid Storage and Determines Metabolic Flexibility. *Cell Rep.* **24**, 2005-2012.e7 (2018).

Acknowledgments: We thank Buck Samuel and Gary Ruvkun for bacterial isolates; Long Ma, Keith Choe, Derek Sieburth, Bob Horvitz, Na An, and the *Caenorhabditis* Genetic Center, which is funded by the NIH National Center for Research Resources (NCRR), for strains; Martin Welch and George Salmond for use of bacterial culture equipment and space, and Martin Hemberg for feedback on RNA-seq analysis. N.O.B is funded by a Next Generation Fellowship from the Centre for Trophoblast Research. C.R. was supported by a Wellcome PhD programme. J.W., A.K. and B.J are funded by BBSRC grant BB/M027252/1. This work was also supported by Cancer Research UK (C13474/A18583, C6946/A14492) and the Wellcome Trust (104640/Z/14/Z, 092096/Z/10/Z) grants to E.A.M.

Competing interests: The authors declare that they have no competing interests.

Data and materials availability: All relevant data are available from the authors on reasonable request and/or are included with the manuscript.

Materials and Methods

Strains. *C. elegans* strains were cultured as described (*34*) and maintained at 20 °C unless noted otherwise. The Bristol strain N2 was the wild-type strain. Mutations used were:

LGI: *set-32(ok1457), prg-1(n4357), spr-5(by134), wdr-23(bur7, bur8, bur9, bur10, tm1817, mac51)*

LGII: *cysl-2(ok3516, syb1431), damt-1(gk961032), rhy-1(n5500, ok1402, tm12398))*

LGIII: *wdr-5.1(ok1417), hrde-1(tm1200), set-2(ok952), met-2(n4256)*

LGIV: *pmk-1(km25), skn-1(zj15), pgl-1(bn102), lin-45(n2018), nIs470[cysl-2::Venus; myo-2::RFP]*

LGV: *egl-9(n586), hif-1(ia4)*

LGX: *cysl-1(ok762, mr23, mr25, mr26, mr29, mr39, mr40)*

Unknown linkage: *burIs2[gst-31::gfp]*

Extrachromosomal arrays: *nEx1763[rhy-1(+); myo-2::RFP], burEx1 [cysl-2(+); myo-3::RFP]*

Sequencing of Pseudomonas vranovensis *BIGb446 and BIGb468*

Genomic DNA was prepped using a Gentra Puregene kit (QIAGEN). DNA was sheared to 10 kb using gTUBE (Covaris). Sheared DNA was barcoded and multiplexed for PacBio sequencing using Template Prep Kit 1.0-SPv3 and Barcoded Adapter Kit 8A (PacBio). Genomic DNA was sequenced using the PacBio Sequel system using version 3.0 sequencing reagents (PacBio) and 1M v3 SMRT cell.

Genome assembly of BIGb446 and BIGb468

The genomes of BIGb446 and BIGb46 were assembled using HGAP4 from SMRT Link version 5.1.0.26412 with estimated genome sizes of 5 MB.

Genomic DNA alignment

MUMmer (*Version 3.0, default parameters*) and MUMmer-plot (*35*) were used to visualize global alignments of BIGb446 and BIGb468 whole genome assemblies. Further to this NUCmer (*35*) and the associated dnadiff script was used to produce statistics on the alignment of the two bacterial genomes.

Assays of adaptation to Pseudomonas vranovensis *BIGb446 and BIGb468*

P. vranovensis BIGb446 and BIGb468 was cultured in LB at 37 °C overnight. 1 mL of overnight culture was seeded onto 50 mm NGM agar plates and dried in a laminar flow hood

(bacterial lawns completely covered the plate such that animals could not avoid the pathogen). All plates seeded with BIGb446 or BIGb468 were used the same day they were seeded. Young adult animals were placed onto 50 mm NGM agar plates seeded with 1 mL either *E. coli* HB101 or *P. vranovensis* BIGb446 or BIGb468 for 24 hours at room temperature. Embryos from these animals were collected and placed onto fresh NGM agar plates seeded with BIGb446 or BIGb468. Percent surviving were counted after 24 hours at room temperature unless otherwise noted.

Transgenerational adaptation to P. vranovensis

P. vranovensis BIGb446 was cultured in LB at 37 °C overnight. 1 mL of overnight culture was seeded onto 50 mm NGM agar plates and dried in a laminar flow hood (bacterial lawns completely covered the plate). All plates seeded with BIGb446 were used the same day they were seeded. All animals in each generation were grown from embryos to young adults on NGM agar plates seeded with *E. coli* HB101. Young adults were then moved to fresh plates seeded with BIGb446 at room temperature for 24 hours. 24 hours of feeding on BIGb446 was counted as one generation of exposure to a BIGb446 diet. Embryos from parents fed BIGb446 were collected and placed onto plates seeded with *E. coli* HB101 until they were young adults and then moved to fresh plates seeded with BIGb446 for additional generations.

Imaging of wild-type animals surviving after P. vranovensis *exposure*

1,000 embryos were placed onto NGM agar plates seeded with *P. vranovensis* BIGb446 at t = 0 in each condition and surviving animals at 120 hours were washed off of plates and resuspended in 20 μl M9 and imaged.

Assays of C. elegans response to P. aeruginosa *and* P. luminescens

Young adult animals were placed onto slow-killing assay (*P. aeruginosa*) plates or NGM agar (*P. luminescens*) plates seeded with either *P. aeruginosa* PA14 or *P. luminescens* Hb for 24 hours at room temperature. Embryos from these animals were collected and snap frozen in liquid nitrogen for RNA sequencing and metabolomics analysis or placed onto fresh NGM agar plates seeded with BIGb446. Percent of animals placed on BIGb446 surviving were counted after 24 hours at room temperature.

Assay of adult survival

Greater than 100 young adult animals were placed onto placed onto NGM agar plates seeded with *P. vranovensis* BIGb446 from overnight cultures in LB. Percent of animals surviving was counted at 24 hour intervals. Animals were scored as alive if they were mobile and dead if they were immobile and did not respond to touch.

RNA-seq

Young adult animals were placed onto NGM agar plates seeded with *E. coli* HB101, *P. vranovensis* BIGb446 or BIGb468, or *P. luminescens* Hb or slow-killing assay plates seeded with *P. aeruginosa* PA14 for 24 hours at room temperature. Adult animals or embryos collected from adult animals after 24 hours were snap frozen in liquid nitrogen. Samples were lysed using a BeadBug microtube homogenizer (Sigma) and 0.5 mm Zirconium beads (Sigma). RNA was extracted using a RNeasy Plus Mini kit (Qiagen). mRNA was enriched using an NEBNext rRNA Depletion kit (NEB). Libraries for sequencing were prepped using an NEBNext Ultra II Library prep kit for Illumina (NEB) and loaded for paired-end sequencing using the Illumina HiSeq 1500.

RNA-seq and principal component analysis

Cutadapt version 1.18 was used to remove adapter sequences (AATGATACGGCGACCACCGAGATCTACACTCTTTCCCTACACGACGCTCTTCCGATC for HS678 and AGATCGGAAGAGCACACGTCTGAACTCCAGTCA (forward) and AGATCGGAAGAGCGTCGTGTAGGGAAAGAGTGT (reverse) for HS755. Cutadapt was also used to trim the 3' ends of reads when the phred quality value was below 20. Reads shorter than 40 bp were discarded. The genome sequence in FASTA format and annotation file in GFF3 format of *C. elegans* were downloaded from Ensembl release 96. The genome sequence was index with the annotation with hisat2 version 2.1.0. hisat2 was used for aligning reads to the reference genome and the maximum number of alignments to be reported per read was set to 5000.Featurecounts from the conda subread package version 1.6.3 was used to count the number of reads per gene. The Ensembl release 96 annotation file in GTF format for *C. elegans* was used. Fragments were counted when they overlapped an exon by at least 1 nucleotide and fragments are reported at the gene level. The option for the stranded protocol was turned off. Only read pairs that had both ends aligned were counted. Given our average fragment length of 300 bp, a distance of between 50 and 600 nucleotides was tolerated for read pairs. Read pairs that had their two ends mapping to different chromosomes or mapping to the same chromosome but on different strands were not counted. Multi-mapping reads were not counted.The raw counts table was imported into R 3.5.1 for differential expression analysis with DESeq2 version 1.22.1 Normalisation was carried out within each contrast. The PCA plots were produced with DESeq2 function plotPCA() after variance stabilising transformation of the data. All code relating to the RNA-seq analysis and the genome assembly and annotation can be found at https://github.com/cristianriccio/celegans-pathogen-adaptation

Mutagenesis screening

Approximately 20,000 L4 stage animals expressing *gst-31::GFP* (*burIs2*) were incubated with 20 μL of EMS in 4 mL of M9 for 4 h at 20 °C, and approximately 200,000 F3 generation embryos were placed onto NGM agar Petri plates seeded with *E. coli* HB101 and screened for mutants that expressed *gst-31::GFP* even in the absence of pathogen infection.

gst-31::GFP *imaging*

To image adults and embryos, young adult animals expressing *burIs2* were placed onto NGM agar plates seeded with BIGb446 at room temperature for 24 hours. Adults and embryos were collected and immediately imaged using a Zeiss AXIO imager A1 microscope and a Hamamatsu ORCA-ER camera.

cysl-2::GFP *imaging*

To image adults and embryos, young adult animals expressing *nIs470* were placed onto NGM agar plates seeded with BIGb446 at room temperature for 24 hours. Embryos were collected and immediately imaged using a Zeiss AXIO imager A1 microscope and a Hamamatsu ORCA-ER camera.

UV-killing bacteria

1 mL of overnight culture of BIGb446 was seeded onto 50 mm NGM agar plates and dried in the laminar flow hood. Seeded plates were then exposed to 20 $\mu W/cm^2$ for 1 hour. Complete killing of bacteria was confirmed by testing inoculations of bacteria in LB overnight.

cysl-2 *cloning and rescue*

Genomic *cysl-2* DNA was amplified from wild-type animals using the primers ACGATTGGGTTGGCTGTAAG and GGTCGTACGTGTTCGTTGTG. Extrachromosomal

arrays were generated by injecting the corresponding PCR fragment and co-injection marker into the gonad of one-day old adults at the specified concentrations. *nobEx1* was generated by injecting *cysl-2* genomic DNA at 20 ng/µl and *myo-3::RFP* was injected at 10 ng/µl. Final injection DNA concentration was brought up to 150 ng/µl using DNA ladder (1kb HyperLadder – Bioline).

Generation of cysl-2 *CRISPR alleles*

syb1431 was generated by SunyBiotech. *syb1431* contains a 50 bp frameshift deletion in the first exon with the following flanking sequences ACCGGTGGTGAGCTCATCGGAAACACCCCA and GGTAGAGTACATGAACCCTGCCTGCTC.

LC/MS lipid profiling

C. elegans was prepared for LC-MS lipidomics and acyl-carnitine analysis as previously described (*36*) with minor modifications. Briefly, ~40 µL of concentrated embryos were re-suspended in 100 µL of water, then 0.4 mL of chloroform was added to each sample followed by 0.2 mL of methanol containing the stable isotope labelled acyl-carnitine internal standards (Butyryl-L-carnitine$_{-d7}$ at 5 µM and Hexadecanoyl-L-carnitine$_{-d3}$ at 5 µM). The samples were then homogenised by vortexing then transferred into a 2 mL Eppendorf screw-cap tube. The original container was washed out with 0.5 mL of chloroform: methanol (2: 1, respectively) and added to the appropriate 2 mL Eppendorf screw-cap tube. This was followed by the addition of 150 µL of the following stable isotope labelled internal standards (approximately 10 to 50 µM in methanol): Ceramide_C16$_{d31}$, LPC_(C14:0$_{d42}$), PC_(C16:0$_{d31}$ / C18:1), PE_(C16:0$_{d31}$ / C18:1), PG_(C16:0$_{d31}$ / C18:1), PI_(C16:0$_{d31}$ / C18:1), PS_(C16:0$_{d62}$),

SM_(C16:0$_{d31}$), TG_(45:0$_{d29}$) and TG_(48:0$_{d31}$). Then, 400 µL of sterile water was added. The samples were vortexed for 1 min, and then centrifuged at ~20,000 rpm for 5 minutes.

For the intact lipid sample preparation, 0.3 mL of the organic layer (the lower chloroform layer) was collected into a 2 mL amber glass vial (Agilent Technologies, Santa Clara California, USA) and dried down to dryness in an Eppendorf Concentrator Plus system (Eppendorf, Stevenage, UK) run for 60 minutes at 45 °C. The dried lipid samples were then reconstituted with 100 µL of 2:1:1 solution of propan-2-ol, acetonitrile and water, respectively, and then vortexed thoroughly. The lipid samples were then transferred into a 300 µL low-volume vial insert inside a 2 mL amber glass auto-sample vial ready for liquid chromatography separation with mass spectrometry detection (LC-MS) of intact lipid species.

For the acyl-carnitine sample preparation, 0.2 mL of the organic layer (the lower chloroform layer) and 0.2 mL of the aqueous layer (the top water layer) were mixed into a 2 mL amber glass vial and dried down to dryness. The dried acyl-carnitine samples were then reconstituted with 100 µL of water and acetonitrile (4: 1, respectively) and thoroughly vortexed. The acyl-carnitine samples were then transferred into a 300 µL low-volume vial insert inside a 2 mL amber glass auto-sample vial ready for liquid chromatography separation with mass spectrometry detection (LC-MS) of the acyl-carnitine species.

Full chromatographic separation of intact lipids (*37*) was achieved using Shimadzu HPLC System (Shimadzu UK Limited, Milton Keynes, United Kingdom) with the injection of 10 µL onto a Waters Acquity UPLC® CSH C18 column; 1.7 µm, I.D. 2.1 mm X 50 mm, maintained at 55 °C. Mobile phase A was 6:4, acetonitrile and water with 10 mM ammonium formate. Mobile phase B was 9:1, propan-2-ol and acetonitrile with 10 mM ammonium formate. The

flow was maintained at 500 µL per minute through the following gradient: 0.00 minutes_40% mobile phase B; 0.40 minutes_43% mobile phase B; 0.45 minutes_50% mobile phase B; 2.40 minutes_54% mobile phase B; 2.45 minutes_70% mobile phase B; 7.00 minutes_99% mobile phase B; 8.00 minutes_99% mobile phase B; 8.3 minutes_40% mobile phase B; 10 minutes_40% mobile phase B; 10.00 minutes_40% mobile phase B. The sample injection needle was washed using 9:1, 2-propan-2-ol and acetonitrile with 0.1 % formic acid. The mass spectrometer used was the Thermo Scientific Exactive Orbitrap with a heated electrospray ionisation source (Thermo Fisher Scientific, Hemel Hempstead, UK). The mass spectrometer was calibrated immediately before sample analysis using positive and negative ionisation calibration solution (recommended by Thermo Scientific). Additionally, the heated electrospray ionisation source was optimised at 50:50 mobile phase A to mobile phase B for spray stability (capillary temperature; 380 °C, source heater temperature; 420 °C, sheath gas flow; 60 (arbitrary), auxiliary gas flow; 20 (arbitrary), sweep gas; 5 (arbitrary), source voltage; 3.5 kV. The mass spectrometer resolution was set to 25,000 with a full-scan range of m/z 100 to 1,800 Da, with continuous switching between positive and negative mode. Lipid quantification was achieved using the area under the curve (AUC) of the corresponding high resolution extracted ion chromatogram (with a window of ± 8 ppm) at the indicative retention time. The lipid analyte AUC relative to the associated internal standard AUC for that lipid class was used to semi-quantify and correct for any extraction/instrument variation.

Acyl-carnitine chromatographic separation was achieved using an ACE Excel 2 C18-PFP (150 mm, I.D. 2.1 mm, 2 µm) LC-column with a Shimadzu UPLC system. The column was maintained at 55 ^{o}C with a flow rate of 0.5 mL/min. A binary mobile phase system was used with mobile phase A; water (with 0.1% formic acid), and mobile phase B; acetonitrile (with 0.1% formic acid). The gradient profile was as follows; at 0 minutes_0% mobile phase B, at

0.5 minutes_100% mobile phase B, at 5.5 minutes_100% mobile phase B, at 5.51 minutes_0% mobiles phase B, at 7 minutes_0% mobile phase B. Mass spectrometry detection was performed on a Thermo Exactive orbitrap mass spectrometer operating in positive ion mode. Heated electrospray source was used; the sheath gas was set to 40 (arbitrary units), the aux gas set to 15 (arbitrary units) and the capillary temperature set to 250°C. The instrument was operated in full scan mode from m/z 75–1000 Da. Acyl-carnitine quantification was achieved using the area under the curve (AUC) of the corresponding high resolution extracted ion chromatogram (with a window of ± 8 ppm) at the indicative retention time. The acyl-carnitine analyte AUC relative to the associated internal standard AUC was used to semi-quantify and correct for any extraction/instrument variation. All lipid values were normalized to total lipid.

Data availability

Genomic DNA and RNA-seq data that support the findings of this study have been deposited at the European Nucleotide Archive under the accession code PRJEB32993. Raw data supporting all figures is provided in Supplementary Table 6. All other relevant data are available from the authors on reasonable request and/or are included with the manuscript.

Statistics and reproducibility

ANOVA analysis with post hoc p-value calculations was used for Fig. 1A, 1E, 1F, 1G, 3D, 4D, 4E, 4F, 4G, Supplementary Fig. 1B and 3. Two-tail t-tests were used for Fig. 1B, 1D, 4A, 4B, Supplementary Fig. 1A and 1C. For Fig. 2B, 2D, and 3E the *p*-value was calculated using a normal approximation to the hypergeometric probability, as in http://nemates.org/MA/progs/representation.stats.html. For lipidomics data p-values were calculated using two-tail t-tests and statistical significance was determined using Bonferonni correction for multiple hypotheses. * = $p < 0.05$, ** = $p < 0.01$, *** = $p < 0.001$, **** $p <$

0.0001. No statistical method was used to predetermine sample size. The experiments were not randomized. The investigators were not blinded to allocation during experiments and outcome assessment.

Methods References

1. N. O. Burton *et al.*, Insulin-like signalling to the maternal germline controls progeny response to osmotic stress. *Nat. Cell Biol.* **19**, 252–257 (2017).

2. B. Dantzer *et al.*, Density triggers maternal hormones that increase adaptive offspring growth in a wild mammal. *Science*. **340**, 1215–1217 (2013).

3. N. N. Vellichirammal, P. Gupta, T. A. Hall, J. A. Brisson, Ecdysone signaling underlies the pea aphid transgenerational wing polyphenism. *Proc. Natl. Acad. Sci. U. S. A.* **114**, 1419–1423 (2017).

4. O. Roth *et al.*, Paternally derived immune priming for offspring in the red flour beetle, Tribolium castaneum. *J. Anim. Ecol.* **79**, 403–413 (2010).

5. W. D. Hamilton, R. Axelrod, R. Tanese, Sexual reproduction as an adaptation to resist parasites (a review). *Proc. Natl. Acad. Sci. U. S. A.* **87**, 3566–3573 (1990).

6. T. J. Little, A. R. Kraaijeveld, Ecological and evolutionary implications of immunological priming in invertebrates. *Trends Ecol. Evol.* **19**, 58–60 (2004).

7. J. Dhinaut, M. Chogne, Y. Moret, Immune priming specificity within and across generations reveals the range of pathogens affecting evolution of immunity in an insect. *J. Anim. Ecol.* **87**, 448–463 (2018).

8. F. Yue *et al.*, Maternal transfer of immunity in scallop Chlamys farreri and its trans-generational immune protection to offspring against bacterial challenge. *Dev. Comp. Immunol.* **41**, 569–577 (2013).

9. C. C. Huang, Y. L. Song, Maternal transmission of immunity to white spot syndrome associated virus (WSSV) in shrimp (Penaeus monodon). *Dev. Comp. Immunol.* **23**, 545–552 (1999).

10. E. Luna, T. J. A. Bruce, M. R. Roberts, V. Flors, J. Ton, Next-generation systemic acquired resistance. *Plant Physiol.* **158**, 844–853 (2012).

11. L. A. Hanson *et al.*, The transfer of immunity from mother to child. *Ann. N. Y. Acad. Sci.* **987**, 199–206 (2003).

12. B. S. Samuel, H. Rowedder, C. Braendle, M.-A. Felix, G. Ruvkun, Caenorhabditis elegans responses to bacteria from its natural habitats. *Proc. Natl. Acad. Sci. U. S. A.* **113**, E3941-3949 (2016).

13. M. Gomila, A. Pena, M. Mulet, J. Lalucat, E. Garcia-Valdes, Phylogenomics and systematics in Pseudomonas. *Front. Microbiol.* **6**, 214 (2015).

14. P. N. Tran, M. A. Savka, H. M. Gan, In-silico Taxonomic Classification of 373 Genomes Reveals Species Misidentification and New Genospecies within the Genus Pseudomonas. *Front. Microbiol.* **8**, 1296 (2017).

15. S.-H. Yoon, S.-M. Ha, J. Lim, S. Kwon, J. Chun, A large-scale evaluation of algorithms to calculate average nucleotide identity. *Antonie Van Leeuwenhoek*. **110**, 1281–1286 (2017).

16. L. Tvrzova *et al.*, Pseudomonas moraviensis sp. nov. and Pseudomonas vranovensis sp. nov., soil bacteria isolated on nitroaromatic compounds, and emended description of Pseudomonas asplenii. *Int. J. Syst. Evol. Microbiol.* **56**, 2657–2663 (2006).

17. E. L. Greer *et al.*, Transgenerational epigenetic inheritance of longevity in Caenorhabditis elegans. *Nature*. **479**, 365–371 (2011).

18. C. Ma *et al.*, N6-methyldeoxyadenine is a transgenerational epigenetic signal for mitochondrial stress adaptation. *Nat. Cell Biol.* **21**, 319–327 (2019).

19. R. S. Moore, R. Kaletsky, C. T. Murphy, Piwi/PRG-1 Argonaute and TGF-β Mediate Transgenerational Learned Pathogenic Avoidance. *Cell* (2019), doi:10.1016/j.cell.2019.05.024.

20. B. A. Buckley *et al.*, A nuclear Argonaute promotes multigenerational epigenetic inheritance and germline immortality. *Nature*. **489**, 447–451 (2012).

21. A. Ashe *et al.*, piRNAs can trigger a multigenerational epigenetic memory in the germline of C. elegans. *Cell*. **150**, 88–99 (2012).

22. I. Lev *et al.*, MET-2-Dependent H3K9 Methylation Suppresses Transgenerational Small RNA Inheritance. *Curr. Biol. CB*. **27**, 1138–1147 (2017).

23. D. D. Bolz, J. L. Tenor, A. Aballay, A conserved PMK-1/p38 MAPK is required in caenorhabditis elegans tissue-specific immune response to Yersinia pestis infection. *J. Biol. Chem.* **285**, 10832–10840 (2010).

24. D. H. Kim *et al.*, A conserved p38 MAP kinase pathway in Caenorhabditis elegans innate immunity. *Science*. **297**, 623–626 (2002).

25. I. Engelmann *et al.*, A comprehensive analysis of gene expression changes provoked by bacterial and fungal infection in C. elegans. *PloS One*. **6**, e19055 (2011).

26. M. A. Jobson *et al.*, Transgenerational Effects of Early Life Starvation on Growth, Reproduction, and Stress Resistance in Caenorhabditis elegans. *Genetics*. **201**, 201–212 (2015).

27. N. O. Burton *et al.*, Neurohormonal signaling via a sulfotransferase antagonizes insulin-like signaling to regulate a Caenorhabditis elegans stress response. *Nat. Commun.* **9**, 5152 (2018).

28. L. Tang, W. Dodd, K. Choe, Isolation of a Hypomorphic skn-1 Allele That Does Not Require a Balancer for Maintenance. *G3 Bethesda Md*. **6**, 551–558 (2015).

29. T. A. Staab *et al.*, The conserved SKN-1/Nrf2 stress response pathway regulates synaptic function in Caenorhabditis elegans. *PLoS Genet.* **9**, e1003354 (2013).

30. Z. Xu *et al.*, WDR-23 and SKN-1/Nrf2 Coordinate with the BLI-3 Dual Oxidase in Response to Iodide-Triggered Oxidative Stress. *G3 Bethesda Md*. **8**, 3515–3527 (2018).

31. K. P. Choe, A. J. Przybysz, K. Strange, The WD40 repeat protein WDR-23 functions with the CUL4/DDB1 ubiquitin ligase to regulate nuclear abundance and activity of SKN-1 in Caenorhabditis elegans. *Mol. Cell. Biol.* **29**, 2704–2715 (2009).

32. D. K. Ma, R. Vozdek, N. Bhatla, H. R. Horvitz, CYSL-1 interacts with the O2-sensing hydroxylase EGL-9 to promote H2S-modulated hypoxia-induced behavioral plasticity in C. elegans. *Neuron*. **73**, 925–940 (2012).

33. M. W. Budde, M. B. Roth, The response of Caenorhabditis elegans to hydrogen sulfide and hydrogen cyanide. *Genetics*. **189**, 521–532 (2011).

34. S. Brenner, The genetics of Caenorhabditis elegans. *Genetics*. **77**, 71–94 (1974).

35. S. Kurtz *et al.*, Versatile and open software for comparing large genomes. *Genome Biol.* **5**, R12 (2004).

36. J. FOLCH, M. LEES, G. H. SLOANE STANLEY, A simple method for the isolation and purification of total lipides from animal tissues. *J. Biol. Chem.* **226**, 497–509 (1957).

37. S. Virtue *et al.*, Peroxisome Proliferator-Activated Receptor gamma2 Controls the Rate of Adipose Tissue Lipid Storage and Determines Metabolic Flexibility. *Cell Rep.* **24**, 2005-2012.e7 (2018).

Figure 1. *C. elegans* transgenerationally adapts to infection by *Pseudomonas vranovensis.*

(A) Percent of wild-type animals surviving on plates seeded with either *E. coli* HB101 or bacterial isolates BIGb446 and BIGb468 after 24 hrs. Error bars, s.d. n = 3 experiments of

>100 animals. (B) Percent of wild-type animals surviving on plates seeded with bacterial isolate BIGb446. Error bars, s.d. n = 3 experiments of 500 animals. (C) Images of wild-type animals surviving after 120 hrs of feeding on bacterial isolate BIGb446. 1000 animals were used at t = 0 in each condition and surviving animals were resuspended in 20 μl M9 and imaged. Scale bars 1 mm. (D) Percent of wild-type animals surviving on *E. coli* HB101 or bacterial isolate BIGb446 after 24 hrs. Error bars, s.d. n = 3 experiments of >100 animals. (E) Percent of wild-type animals surviving on plates seeded with bacterial isolate BIGb446 after 24 hrs. Error bars s.d. n = 3 experiments of > 100 animals. (F) Percent of wild-type animals surviving on plates seeded with bacterial isolate BIGb446 after 24 hrs. Error bars s.d. n = 3 experiments of 500 animals. Wild-type animals carried the integrated transgene *nIs470.* (G) Percent of wild-type animals surviving on plates seeded with bacterial isolate BIGb446 after 24 hrs. Error bars s.d. n = 3 experiments of 500 animals. * = $p < 0.05$, ** = $p < 0.01$, *** = $p < 0.001$, **** $p < 0.0001$.

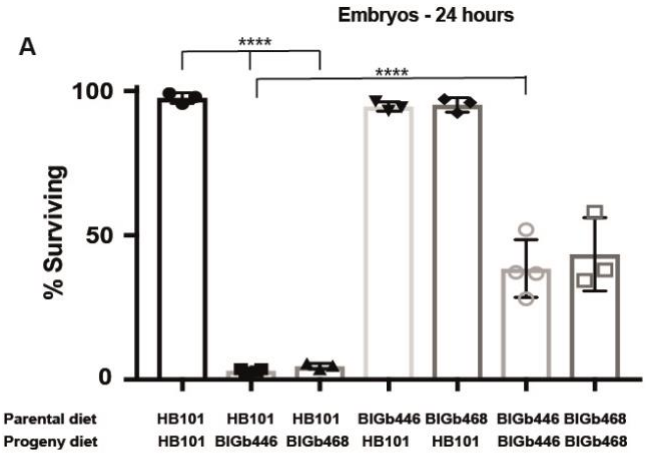
A
Embryos - 24 hours
% Surviving
100
50
0
****
****
Parental diet
Progeny diet
HB101 HB101
HB101 BIGb446
HB101 BIGb468
BIGb446 HB101
BIGb468 HB101
BIGb446 BIGb446
BIGb468 BIGb468

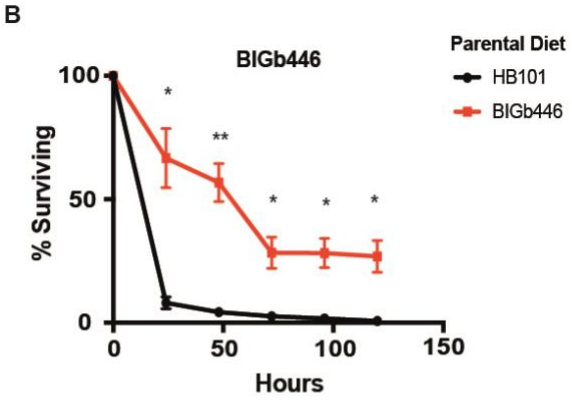
B
BIGb446
Parental Diet
HB101
BIGb446
% Surviving
100
50
0
0
50
100
150
Hours
*
**
*
*
*

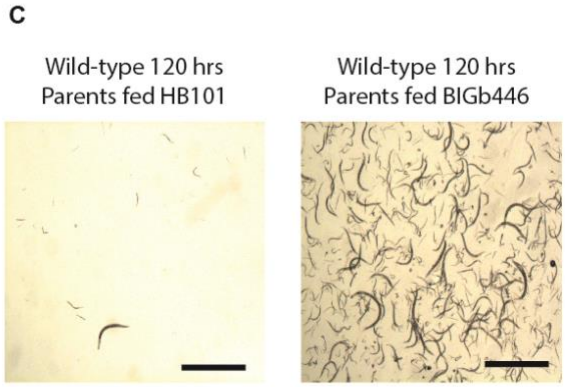
C
Wild-type 120 hrs
Parents fed HB101
Wild-type 120 hrs
Parents fed BIGb446

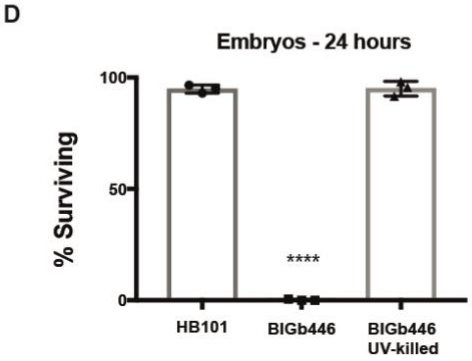
D
Embryos - 24 hours
% Surviving
100
50
0
****
HB101
BIGb446
BIGb446
UV-killed

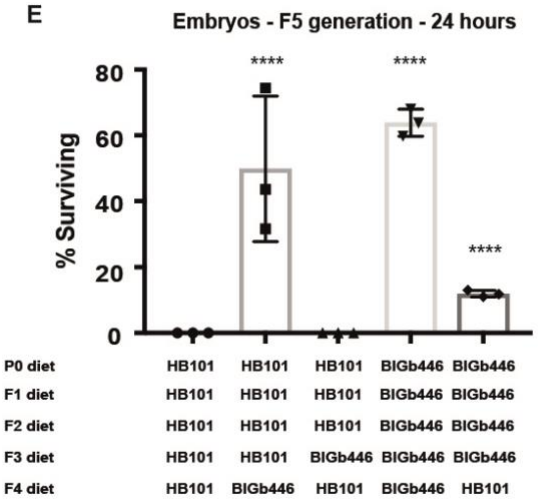
E
Embryos - F5 generation - 24 hours
% Surviving
80
60
40
20
0
****
****
****
P0 diet HB101 HB101 HB101 BIGb446 BIGb446
F1 diet HB101 HB101 HB101 BIGb446 BIGb446
F2 diet HB101 HB101 HB101 BIGb446 BIGb446
F3 diet HB101 HB101 BIGb446 BIGb446 BIGb446
F4 diet HB101 BIGb446 HB101 BIGb446 HB101

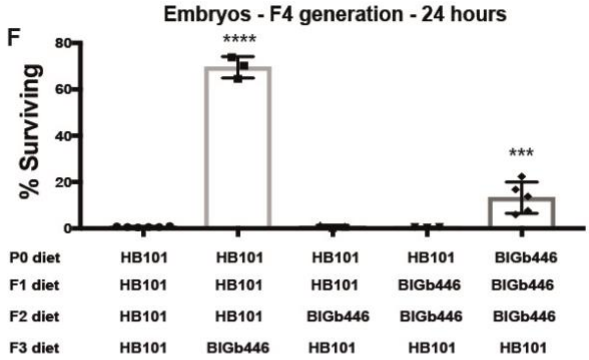
F
Embryos - F4 generation - 24 hours
% Surviving
80
60
40
20
0
****
***
P0 diet HB101 HB101 HB101 HB101 BIGb446
F1 diet HB101 HB101 HB101 BIGb446 BIGb446
F2 diet HB101 HB101 BIGb446 BIGb446 BIGb446
F3 diet HB101 BIGb446 HB101 HB101 HB101

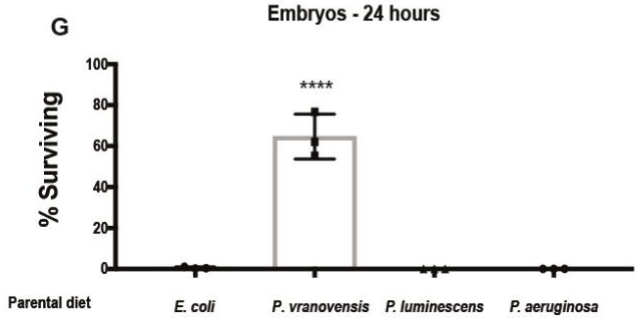
G
Embryos - 24 hours
% Surviving
100
80
60
40
20
0
****
Parental diet
E. coli
P. vranovensis
P. luminescens
P. aeruginosa

Figure 2. Parental infection by *P. vranovensis* alters gene expression and metabolism in offspring. (A) Gene expression changes in embryos from parents fed *P. vranovensis* BIGb446 when compared to embryos from parents fed *E. coli* HB101. Values represent averages from three replicates. (B) Venn diagram of genes exhibiting a greater than 2-fold change in RNA expression in adults fed *P. vranovensis* BIGb446 and embryos from adults fed *P. vranovensis* BIGb446. *p*-value represents normal approximation to the hypergeometric probability (See Statistics and Reproducibility) (C) μM abundance of lipid metabolites exhibiting a greater than 2-fold change in abundance in embryos from parents fed *P. vranovensis* BIGb446 when compared to embryos from parents fed *E. coli* HB101. Error bars, s.d. n = 3 replicates. (D) Venn diagram of genes exhibiting a greater than 2-fold change in RNA expression in embryos from parents fed *P. vranovensis* BIGb446, *P. aeruginosa* PA14, and *P. luminescens* Hb. *p*-value represents normal approximation to the hypergeometric probability (See Statistics and Reproducibility) (E) Principal component analysis (PCA) plot of mRNA expression data from RNA-seq of embryos from parents fed *E. coli* HB101, *P. vranovensis* BIGb446 and BIGb468, *P. aeruginosa* PA14, or *P. luminescens* Hb.

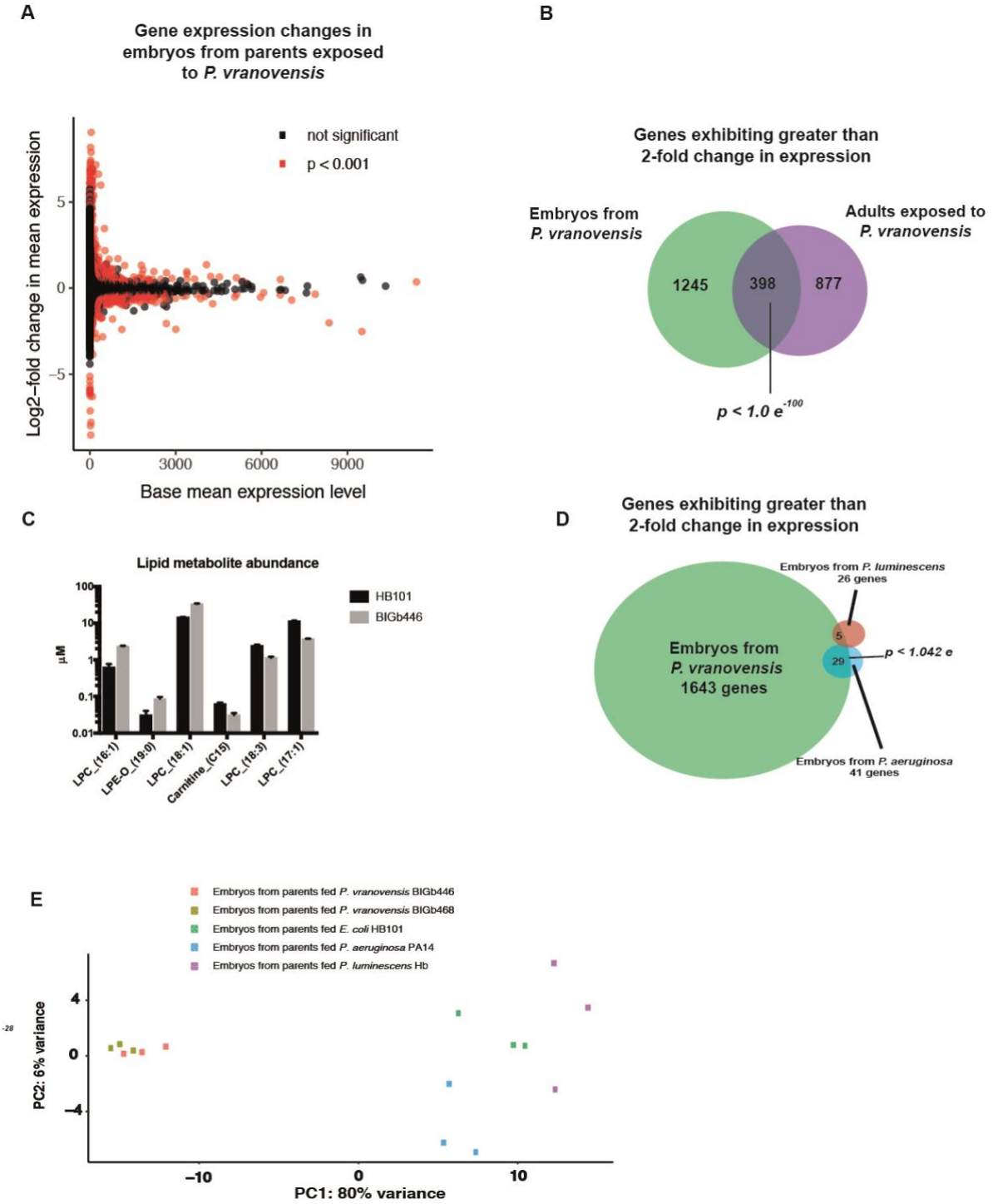
A
Gene expression changes in embryos from parents exposed to P. vranovensis
not significant
p < 0.001
Log2–fold change in mean expression
Base mean expression level
B
Genes exhibiting greater than 2-fold change in expression
Embryos from P. vranovensis
Adults exposed to P. vranovensis
1245
398
877
p < 1.0 e-100
C
Lipid metabolite abundance
HB101
BIGb446
µM
LPC_(16:1)
LPE-O_(19:0)
LPC_(18:1)
Carnitine_(C15)
LPC_(18:3)
LPC_(17:1)
D
Genes exhibiting greater than 2-fold change in expression
Embryos from P. luminescens 26 genes
Embryos from P. vranovensis 1643 genes
p < 1.042 e
Embryos from P. aeruginosa 41 genes
E
Embryos from parents fed P. vranovensis BIGb446
Embryos from parents fed P. vranovensis BIGb468
Embryos from parents fed E. coli HB101
Embryos from parents fed P. aeruginosa PA14
Embryos from parents fed P. luminescens Hb
PC2: 6% variance
PC1: 80% variance

Figure 3. Signaling via WDR-23 regulates *C. elegans* response to *P. vranovensis.* (A) Representative images of *gst-31::GFP* expression in wild-type embryos from parents fed either *E. coli* HB101 or *P. vranovensis* BIGb446. Scale bars 10 μm. (B) Representative images of *gst-31::GFP* expression in wild-type adults fed either *E. coli* HB101 or *P. vranovensis* BIGb446 for 24 hrs. Scale bars 100 μm. (C) Schematic of *wdr-23* mutations that cause increased *gst-31::GFP* expression when animals are fed *E. coli* HB101. Scale bar, 100 bp. (D) Percent of wild-type, *wdr-23(mac51, tm1817),* and *skn-1(zj15)* mutants surviving on plates seeded with bacterial isolates BIGb446 after 24 hrs. Error bars, s.d. n = 3 experiments of >100 animals. **** $p < 0.0001$. (E) Venn diagram of genes exhibiting a greater than 2-fold change in RNA expression in embryos from parents fed *P. vranovensis* BIGb446 and *wdr-23(bur9)* mutant embryos from parents fed *E. coli* HB101. *p*-value represents normal approximation to the hypergeometric probability (See Statistics and Reproducibility). (F) Principal component analysis (PCA) plot of mRNA expression data from RNA-seq of wild-type and *wdr-23(bur9)* mutant embryos from parents fed *E. coli* HB101, *P. vranovensis* BIGb446, *P. aeruginosa* PA14, or *P. luminescens* Hb.

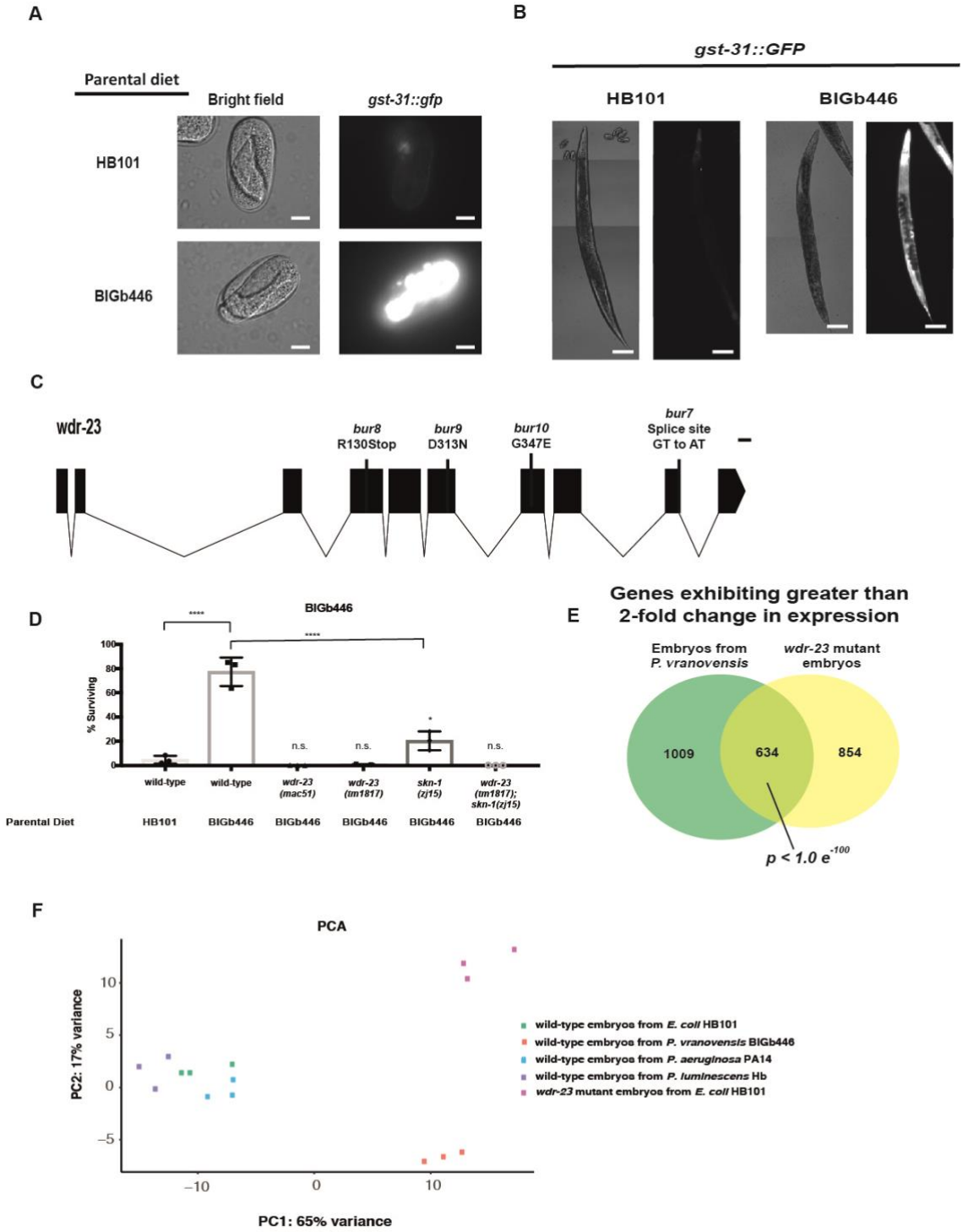
A
Parental diet
Bright field
gst-31::gfp
HB101
BIGb446
B
gst-31::GFP
HB101
BIGb446
C
wdr-23
bur8
R130Stop
bur9
D313N
bur10
G347E
bur7
Splice site
GT to AT
D
BIGb446
% Surviving
****
****
n.s.
n.s.
*
n.s.
wild-type
wild-type
wdr-23 (mac51)
wdr-23 (tm1817)
skn-1 (zj15)
wdr-23 (tm1817); skn-1(zj15)
Parental Diet
HB101
BIGb446
BIGb446
BIGb446
BIGb446
BIGb446
E
Genes exhibiting greater than 2-fold change in expression
Embryos from P. vranovensis
wdr-23 mutant embryos
1009
634
854
p < 1.0 e-100
F
PCA
PC2: 17% variance
PC1: 65% variance
wild-type embryos from E. coli HB101
wild-type embryos from P. vranovensis BIGb446
wild-type embryos from P. aeruginosa PA14
wild-type embryos from P. luminescens Hb
wdr-23 mutant embryos from E. coli HB101

Figure 4. Parental infection by *P. vranovensis* promotes progeny pathogen resistance by increasing the expression of RHY-1, CYSL-1, and CYSL-2 in offspring. (A) Transcripts per million (TPM) of *rhy-1* and *cysl-2* in embryos from parents fed *E. coli* HB101 or *P. vraonvensis* BIGb446. Error bars, s.d. n = 3 replicates. (B) Transcripts per million (TPM) of *rhy-1* and *cysl-2* in embryos from wild-type or *wdr-23(bur9)* mutants. Error bars, s.d. n = 3 replicates. (C) Representative images of *cysl-2::GFP* in embryos from parents fed *E. coli* HB101 or *P. vraonvensis* BIGb446. Scale bars 100 μm. (D) Percent of wild-type and *cysl-2(ok3516)* mutants surviving on plates seeded with bacterial isolates BIGb446 after 24 hrs. Error bars, s.d. n = 3 experiments of >100 animals. (E) Percent of wild-type and *rhy-1* mutants surviving on plates seeded with bacterial isolates BIGb446 after 24 hrs. Error bars, s.d. n = 3 experiments of >100 animals. (F) Percent of wild-type and *cysl-1(ok762)* mutants surviving on plates seeded with bacterial isolates BIGb446 after 24 hrs. Error bars, s.d. n = 3 experiments of >100 animals. (G) Percent of wild-type, *egl-9(n586)*, *hif-1(ia4)*, and *rhy-1(n5500)* mutants surviving on plates seeded with bacterial isolates BIGb446 after 24 hrs. Error bars, s.d. n = 3 experiments of >100 animals. The wild-type data in panels e, f, and g is identical as these experiments were run together. * = $p < 0.05$, ** = $p < 0.01$, *** = $p < 0.001$, **** $p < 0.0001$.

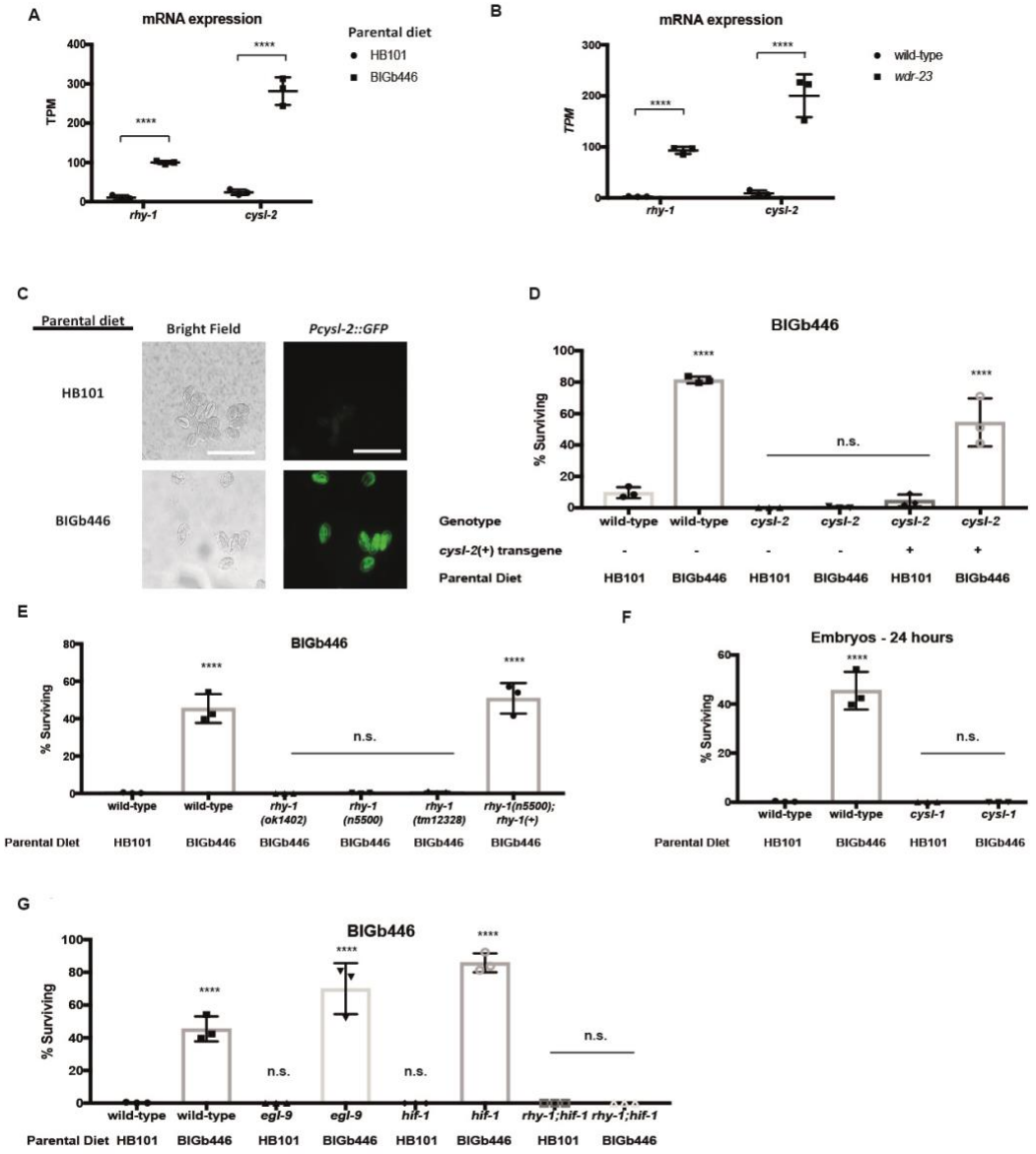
A
mRNA expression
Parental diet
HB101
BIGb446
TPM
rhy-1
cysl-2
B
mRNA expression
wild-type
wdr-23
TPM
rhy-1
cysl-2
C
Parental diet
Bright Field
Pcysl-2::GFP
HB101
BIGb446
D
BIGb446
% Surviving
n.s.
Genotype
cysl-2(+) transgene
Parental Diet
wild-type
cysl-2
HB101
BIGb446
E
BIGb446
% Surviving
n.s.
rhy-1 (ok1402)
rhy-1 (n5500)
rhy-1 (tm12328)
rhy-1(n5500); rhy-1(+)
Parental Diet
F
Embryos - 24 hours
% Surviving
n.s.
cysl-1
Parental Diet
G
BIGb446
% Surviving
n.s.
egl-9
hif-1
rhy-1;hif-1
Parental Diet

Supplementary Figure 1. Genes associated with transgenerational inheritance and pathogen infection in *C. elegans* are not required for heritable adaptation to *P. vranovensis* BIGb446. (A) Percent of wild-type and *pmk-1(km25)* mutant adults surviving on NGM plates seeded with P. vranovenis BIGb446. Error bars, s.d. n = 3 replicates of 100 animals. (B) Percent of wild-type, *set-32(ok1457), prg-1(n4357), hrde-1(tm1200), damt-1(gk961032), wdr-5.1(ok1417), set-2(ok952), spr-5(by134), lin-45(n2018),* and *met-2(n4256)* mutants surviving on plates seeded with bacterial isolates BIGb446 after 24 hrs. Error bars, s.d. n = 3 experiments of >100 animals. (C) Percent of wild-type and *pmk-1(km25)* mutants surviving on plates seeded with bacterial isolates BIGb446 after 24 hrs. Error bars, s.d. n = 3 experiments of >100 animals. * = $p < 0.05$, ** = $p < 0.01$, *** = $p < 0.001$.

A

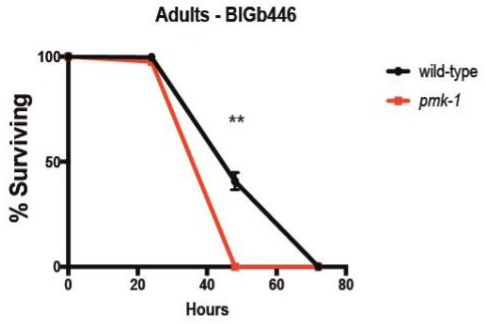
Adults - BIGb446
% Surviving
100
50
0
0
20
40
60
80
Hours
**
wild-type
pmk-1

B

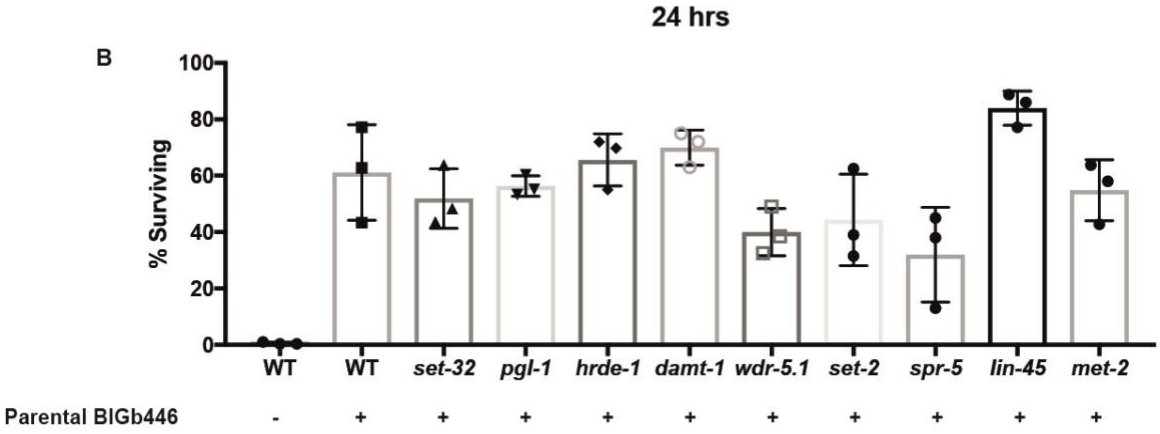
24 hrs
% Surviving
100
80
60
40
20
0
WT
WT
set-32
pgl-1
hrde-1
damt-1
wdr-5.1
set-2
spr-5
lin-45
met-2
Parental BIGb446
-
+
+
+
+
+
+
+
+
+
+

C

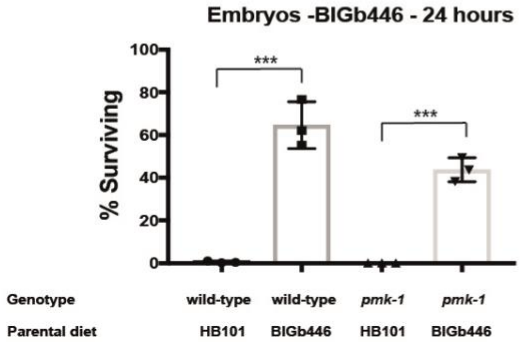
Embryos -BIGb446 - 24 hours
% Surviving
100
80
60
40
20
0
***
***
Genotype
wild-type
wild-type
pmk-1
pmk-1
Parental diet
HB101
BIGb446
HB101
BIGb446

Supplementary Figure 2. BIGb446 and BIGb468 are isolates of a single species. MUMmer plot of the alignments of contigs of BIGb446 and BIGb468 assembled genomes.

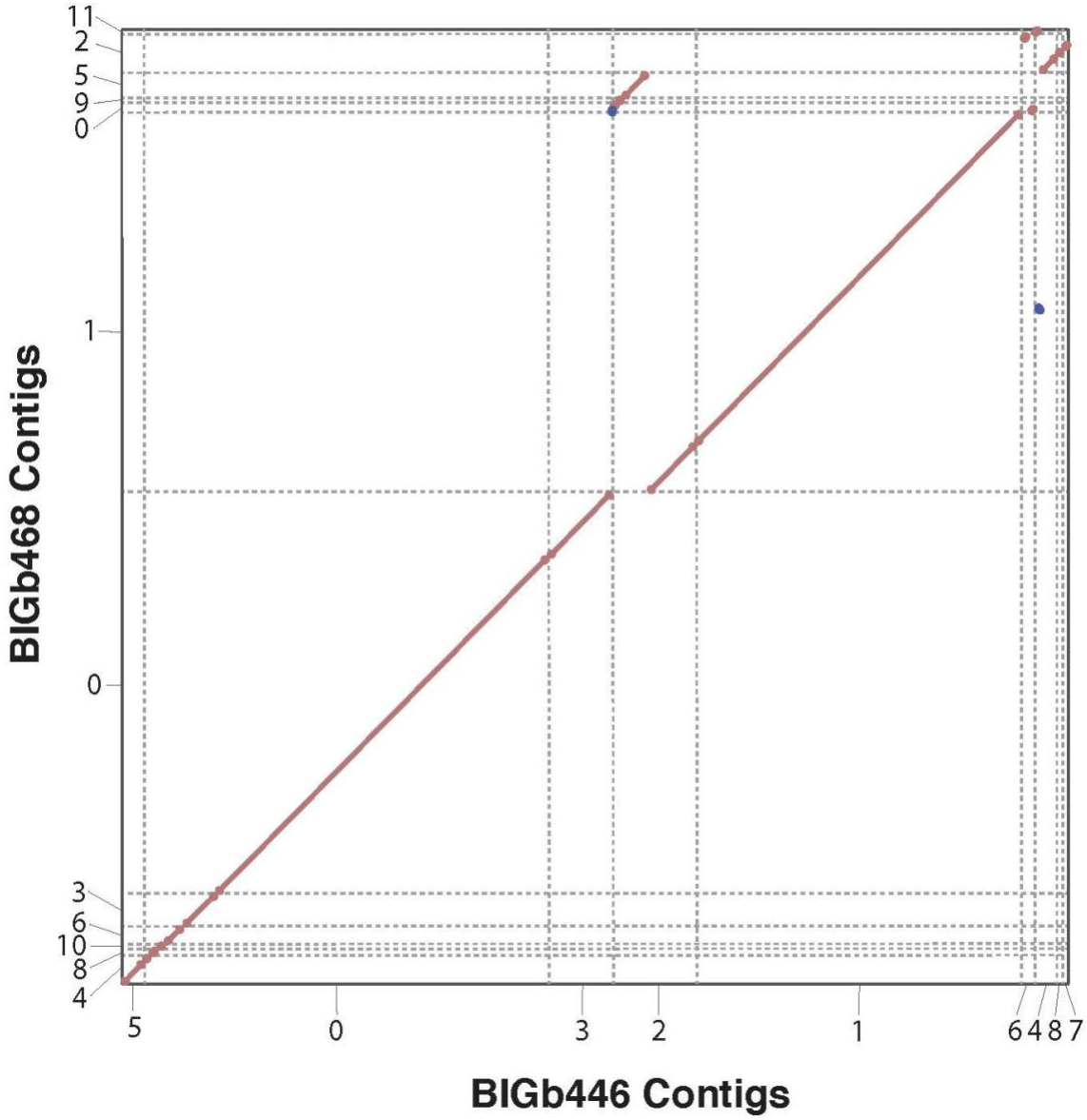
BIGb468 Contigs
BIGb446 Contigs
11
2
5
9
0
1
0
3
6
10
8
4
5
0
3
2
1
6
4
8
7

Supplementary Figure 3. CYSL-1 and CYSL-2 are required for adaptation to *P. vranovensis* BIGb446. Percent of wild-type and *cysl-1(mr23, mr25, mr26, mr29, mr39, mr40)* and *cysl-2(syb1431)* mutants surviving on plates seeded with bacterial isolates BIGb446 after 24 hrs. Error bars, s.d. n = 3 experiments of >100 animals. **** $p < 0.0001$.

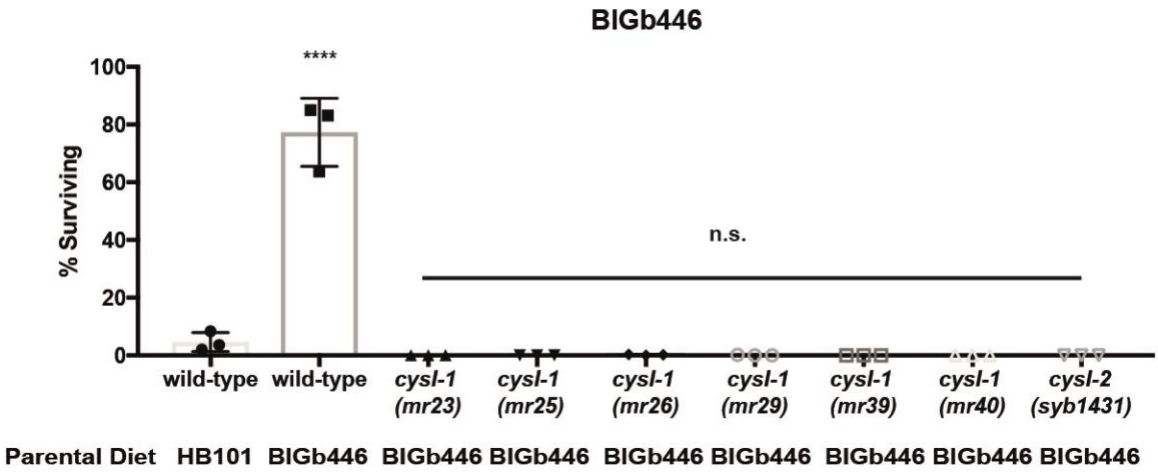
BIGb446
% Surviving
100
80
60
40
20
0
****
n.s.
wild-type
wild-type
cysl-1 (mr23)
cysl-1 (mr25)
cysl-1 (mr26)
cysl-1 (mr29)
cysl-1 (mr39)
cysl-1 (mr40)
cysl-2 (syb1431)
Parental Diet
HB101
BIGb446
BIGb446
BIGb446
BIGb446
BIGb446
BIGb446
BIGb446
BIGb446

Supplementary File 1. Genome assembly of *P. vranovensis* BIGb446. FASTA format file of *P. vranovensis* BIGb446 genomic DNA.

Supplementary File 2. Genome assembly of *P. vranovensis* BIGb468. FASTA format file of *P. vranovensis* BIGb468 genomic DNA.

Supplementary Table 1. Comparison of genomic DNA sequences of BIGb446 and BIGb468 to *P. vranovensis.*

Supplementary Table 2. DEseq2 and TPM analysis of mRNA expression in wild-type embryos from parents fed *E. coli* HB101 or *P. vranovensis* BIGb446.

Supplementary Table 3. Profile of lipid metabolite abundances in wild-type embryos from parents fed *E. coli* HB101 or *P. vranovensis* BIGb446.

Supplementary Table 4. DEseq2 analysis of mRNA expression in wild-type embryos from parents fed *E. coli* HB101, *P. aeruginosa* PA14, or *P. luminescens* Hb.

Supplementary Table 5. DEseq2 analysis of mRNA expression in wild-type and *wdr-23(bur9)* mutant embryos from parents fed *E. coli* HB101. Input for wild-type embryos fed *E. coli* HB101 are the same as Supplementary Table 4 and these samples were analysed at the same time.

Supplementary Table 6. Statistics Source Data